On the Generation of Alfvèn Wave Current Drive in Low Aspect Ratio Tokamaks with Neoclassical Conductivity

C.Bruma, S.Cuperman and K.Komoshvili

School of Physics and Astronomy, Tel Aviv University, 69978 Tel Aviv, Israel

1. Introduction

Several low aspect ratio (spherical) tokamaks (ST's) are now in operation or under construction [1,2]. These devices would permit cost-effective and attractive embodiment of future fusion reactors: they would provide high β, good confinement and steady state operation at modest field values [3] .

Now, a steady state reactor has to be sustained by non-inductively driven currents [4]. Recently, the generation of non-inductive current driven by Alfven waves (AWCD) has been investigated theoretically within the framework of ideal ($E_{||} = 0$) MHD [5,6] and non-ideal, resistive ($E_{||} \neq 0$) MHD [7]; however, in all these cases, the tokamak device consisted of a cylindrical plasma with simulated toroidal effects. Rather encouraging results have been obtained.

In this work we further investigate AWCD in ST's as follows: (i) we use consistent equilibrium profiles with neoclassical conductivity corresponding to an ohmic START discharge [8]; (ii) incorporate effects due to neoclassical conductivity in the elements of the resistive MHD dielectric tensor, in the solution of the full ($E_{||} \neq 0$) wave equation as well as in the calculation of AWCD; and (iii) carry out a systematic search for antenna parameters optimizing the AWCD.

2. Equilibrum profiles and parameters

From the numerical solution of the MHD equations with neoclassical conductivity obtained for START [8], by adequate best fit techniques, we obtain the equilibrium profiles shown in Fig.1. These results correspond to the following START-parameters: inverse aspect ratio, $\varepsilon = 0.697$; elongation of plasma boundary, 1.3; triangularity of plasma boundary, 0.3; toroidal B-field (axis), 0.4895 T; central electron temperature, $T_e(0) = 0.18$ keV; central ion temperature, $T_i(0) = 0.15$ keV; central electron density, $n(0) = 0.25\ 10^{21}\ m^{-3}$. Also, the following profiles are used: current density: $j_0(x) = j_0(0)(1-x)$; $n_e = n_i = n(0)(1-x)^{0.8}$ and $T_l(x) = T_l(0)(1-x)^{0.8}$ ($l = e, i$); here $x \equiv r/a$, a-minor radius. In this work we consider the low field side ($\theta = 0$) simulation of AWCD in START; thus, the problem reduces to a one-dimensional (radial) one, in which, however, essential toroidicity and shear effects are taken into account.

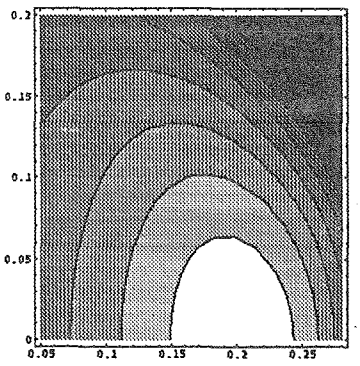

Figure 1: *START equilibrium configuration used in this work: flux surface contours $\Psi_i(R,Z) = C_i$, representing best fits to the numerical results obtained in* [8].

3. Neoclassical conductivity

We have now generalized the previously obtained expressions for current carrying, resistive plasmas [7] by incorporating effects due to neoclassical conductivity. For this, we used the neoclassical conductivity obtained in [9], namely:

$$\frac{\sigma_{nc}}{\sigma_0} = \frac{8}{3\sqrt{\pi}} \int_0^\infty dy\; y^4 e^{-y^4} \left((1 - f_t^\star)\, F_s \left[1 - f_t^\star \left(\nu_D^e \tau_{ee} F_s - 1 \right) \right] \right) , \tag{1}$$

where $\sigma_0 = n_e e^2 \tau_{ee} / m_e$, $\tau_{ee} = 3(4\pi\epsilon_0)^2 m_e^2 v_{th}^3 / \left(16\sqrt{\pi} n_e e^4 \ln\Lambda\right)$ and

$$\nu_D^e(y) = \left(\frac{4}{3\sqrt{\pi}} \tau_{ee} \right)^{-1} \left(\frac{\Phi(y) - G(y) + Z_{eff}}{y^3} \right) . \tag{2}$$

Φ and G are the error function and Chandrasekhar function, respectively:

$$\Phi(y) = \left(\frac{2}{\sqrt{\pi}} \right) \int_0^\infty dy\; e^{-t^2} , \qquad G(y) = \frac{\Phi(y) - y\Phi'(y)}{2y^2} \tag{3}$$

and $f_t^\star$ is the effective trapped particle fraction in the presence of collisions:

$$f_t^\star = f_t \Big(1 + 1.75 \nu_{ee} \left[\nu_D^e(y) \tau_{ee} \right] y^{-1} \Big)^{-1} , \tag{4}$$

where f_t is the trapped particle fraction in the absence of collisions, given by the equation:

$$f_t = 1 - \frac{3}{4} \langle B^2 \rangle \int_0^{1/B_{max}} \frac{\lambda d\lambda}{\langle \sqrt{1 - \lambda B} \rangle} . \tag{5}$$

The Spitzer function, $F_s(Z_{eff}, y)$ is fitted to a polynomial and reads

$$F_s(Z_{eff}, y) = \Lambda_E(Z_{eff}) - \Lambda_T(Z_{eff}) L_1(y^2) + \frac{8}{15} \left(\frac{1}{Z_{eff}} - \Lambda_E(Z_{eff}) + \frac{3}{2} \Lambda_T(Z_{eff}) \right) L_2(y^2) \tag{6}$$

where $L_1(y^2) = (5/2) - y^2$, $L_2(y^2) = (35/8) - (7/2)y^2 + (1/2)y^4$,

$$\Lambda_E(Z_{eff}) = \frac{3.40}{Z_{eff}} \left(\frac{1.13 + Z_{eff}}{2.67 + Z_{eff}} \right) , \quad \Lambda_T(Z_{eff}) = 2.06 \left(\frac{1.38 + Z_{eff}}{3.23 + 4.68 Z_{eff} + {Z_{eff}}^2} \right) . \tag{7}$$

4. The wave equation and its solution

We solved the full (i.e., $E_\parallel \neq 0$) wave equation with the generalized resistive dielectric tensor elements mentioned above, for the case of the low field side plasma configuration represented in Fig.1, in the presence of an external, concentric wave-emitting antenna. In this, appropriate regularity (at $r = 0$) and continuity (at $r = a$) conditions were used. Details of the integration method and its accuracy are found in [7]. Illustrative solutions for the e.m. field components are shown in Figs.3-5.

5. Power absorption and current drive

The time averaged power delivered by the antenna (per unit length) equals the energy flux through the plasma surface:

$$P = -\int_{\Sigma_p} d\Sigma \; Re\left[\frac{c}{8\pi}(\boldsymbol{E}^{\star} \times \boldsymbol{B})\right] = \frac{ac}{4} Re\Big(E_{\|}^{\star} B_{\perp} - E_{\perp}^{\star} B_{\|}\Big)_{r=a} . \tag{8}$$

The locally absorbed power density is

$$p_L(r) \equiv Re(\boldsymbol{E} \cdot \boldsymbol{j}^{*})/2. \tag{9}$$

The AWCD generated in the plasma is [10],

$$j_{0z}^{RF} = j_{0z}^{HI} + j_{0z}^{MT} + j_{0z}^{PF} \tag{10}$$

where ($\eta_{\|} \equiv 1/\sigma_{\|} = m_e \nu_{ei}/1.96ne^2$)

$$j_{0z}^{HI} = \frac{B_{0z}}{2eB_0 n\eta_{\|}\omega}\left\{\frac{B_{0\theta}}{B_0}\frac{1}{r^2}\frac{d}{dr}\left[r^2 \; Re\left(j_r^{*}\frac{E_\theta}{i}\right)\right] + \frac{B_{0z}}{B_0}\frac{1}{r}\frac{d}{dr}\left[r \; Re\left(j_r^{*}\frac{E_z}{i}\right)\right]\right\} \tag{11}$$

$$j_{0z}^{MT} = -\frac{B_{0z}}{2eB_0 n\eta_{\|}\omega}\left\{\frac{B_{0\theta}}{B_0}\frac{m}{r} + \frac{B_{0z}}{B_0}k_z\right\} \; Re\,(\mathbf{E} \cdot \mathbf{j}^{*}) \; , \tag{12}$$

and

$$j_{0z}^{PF} = \frac{B_{0z}}{2eB_0 n\eta_{\|}\omega}\left\{\frac{B_{0\theta}}{B_0}\frac{1}{r^2}\frac{d}{dr}\left[r^2 \; Re\left(j_r^{*}\frac{\omega j_\theta}{\omega_{pe}^2\epsilon_0}\right)\right] + \frac{B_{0z}}{B_0}\frac{1}{r}\frac{d}{dr}\left[r \; Re\left(j_r^{*}\frac{\omega j_z}{\omega_{pe}^2\epsilon_0}\right)\right]\right\} . \tag{13}$$

In these equations, the upperscripts HI, MT and PF indicate, respectively, contributions due to helicity injection, momentum transfer and plasma flow.

6. Results and conclusions

Inspection of the results obtained in this work reveals the following conclusions:

1. For START-like devices considered here, the neoclassical conductivity leads to a small-decrease in the intensities of the field components; correspondingly, a decrease in the current drive occurs (See Fig.2, in which, for illustration $m = 1$, $n = 4$ and $\omega = \omega_{LA}$, the lower edge of the "Alfvèn continuum").

2. There exist well defined (limited) domains in the (m, n) space corresponding to solutions of the wave equation such that a conversion layer exists in the range $0 \leq x \leq 1$; See, e.g., Fig.3 holding for the case $\omega = \omega_{LA}(m, n)$,.

3. The total AWCD is dominated by the MT-component; the maximum integrated MT-component of the AWCD is obtained for relatively small $|n|$ and $|m|$-values; in all cases, the value corresponding to the neoclassical conductivity is smaller than that corresponding to the classical one. (See Fig.4).

4. The total power absorption $P_T \equiv \int dV \; p_L$, is almost unaffected by neoclassical effects and is maximal for small n and $|m|$-values.

5. Finally, for fixed wave numbers ($m = 1$, $n = 4$, for example) the frequency spectrum of the total AWCD reveals the following behaviour: after two large peaks corresponding to

first two GAE's, the absolute value of the total AWCD current increases with the frequency $\bar{\omega} = \omega/\omega_{ci}(0)$, reaching again significant, broad peaks at $\bar{\omega}$-values about 0.5.

References

[1] Sykes, A. *et al.* 1995 *Intern. Conf. on Plasma Physics*, AIP 345.

[2] *Proc. Int. Workshop on Spherical Torus and US-Japan Workshop for Low Aspect Ratio Tokamaks*, 1996, Culham Science and Engineering Center, Abingdon, UK

[3] Peng, Y.-K.M. and Strickler, D. J. 1986 *Nucl. Fusion*, **26**, 769.

[4] Fisch, N. 1987 *Rev. Mod. Phys.*, **59**, 175.

[5] Cuperman, S., Bruma, C., Komoshvili, K. 1996 *J. Plasma Physics*, **56**, part 1, 149.

[6] Komoshvili, K., Cuperman, S. and C.Bruma. 1997 *J. Plasma Physics*, **57**, part 3, 611.

[7] Bruma, C., Cuperman, S. and Komoshvili, K. 1997 *J. Plasma Physics*, in press.

[8] Wilson, H. R., SCENE—Simulation of Self-Consistent Equilibra with Neoclassical Effects, *Fusion Theoretical and Strategic Studies Depart.* Culham Laboratory July, 1994.

[9] Hirshman, S.P. and Sigmar, D. J. 1977, *Physics of Fluids* **20**, 418.

[10] Elfimov, A. G., Petrzilka, V. and Tataronis, J. A. 1994 *Phys. Plasma*, **1**, 2882.

Captions to Figures

Fig.2. Illustrative (normalized) solutions of the full wave equation ($E_{\|} \neq 0$) for the cases of neoclassical (dashed curves) and classical (solid curves) conductivities. *Top:* (a-d) Radial profiles of ReE_N, ImE_N, ReB_N and ImB_N, respectively. *Bottom:* (e-h) Radial profiles of local power deposition and AWCD-components (i.e., plasma flow, helicity injection and momentum transfer), respectively. (Here, $m = 1$, $n = 4$).

Fig.3. (a-d) Computed "Existence Domains" corresponding to sets of (m, n) values, which, for the equilibrium state described in Fig.1, lead to conversion layers situated in the range $0 \leq x \leq 1$.

Fig.4. (m, n)-dependence of the integrated normalized total AWCD (MT+HI+PF); solid (dashed) curves correspond to the classical (neoclassical) conductivity.

Fig.5. Wave-frequency ($\bar{\omega} \equiv \omega/\omega_{ci}(0)$) — dependence of the normalized AWCD-components MT (a), HI (b), PF (c) and of the total AWCD (d). Solid (dashed) curves correspond to classical (neoclassical) conductivity; $m = 1$, $n = 4$.

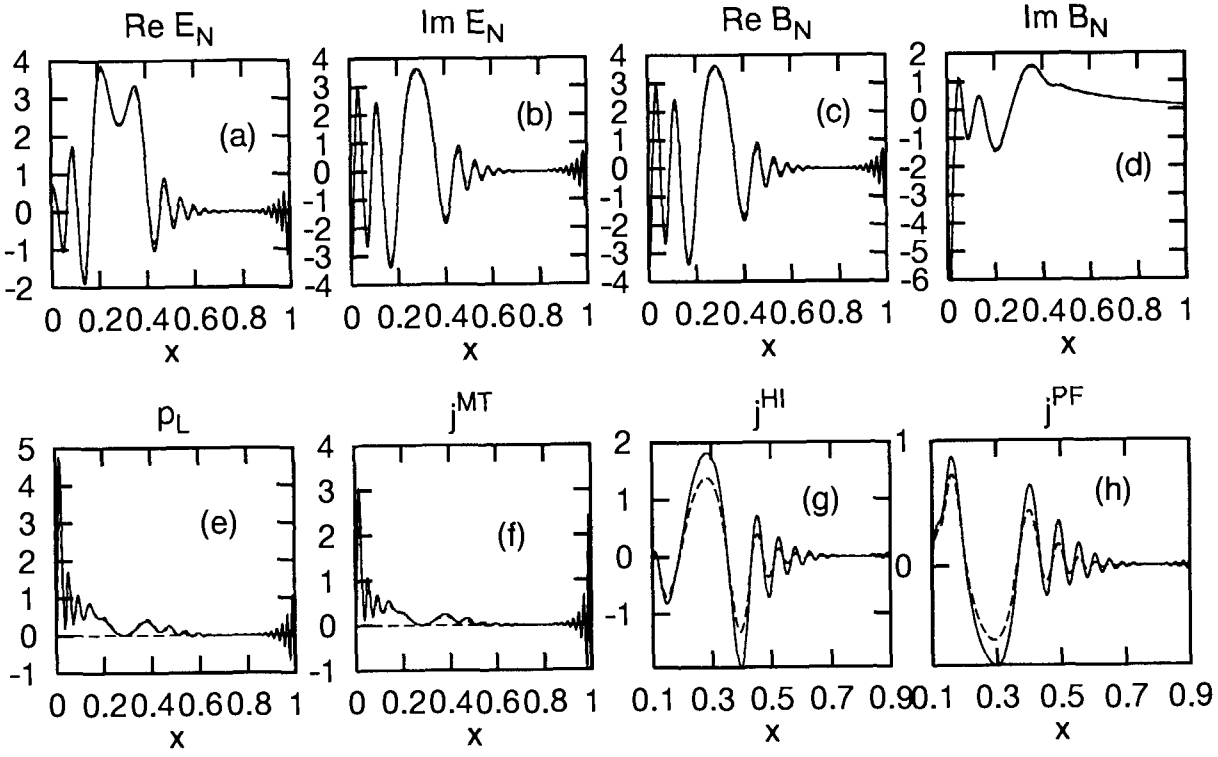

FIG.2

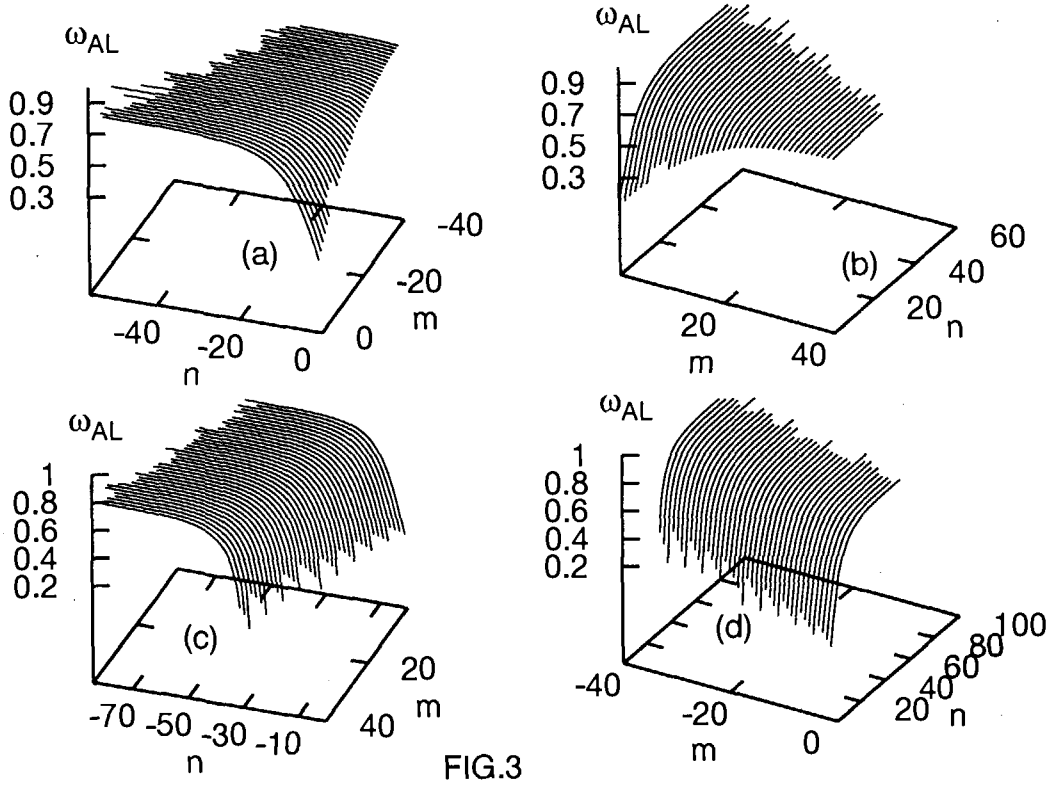

FIG.3

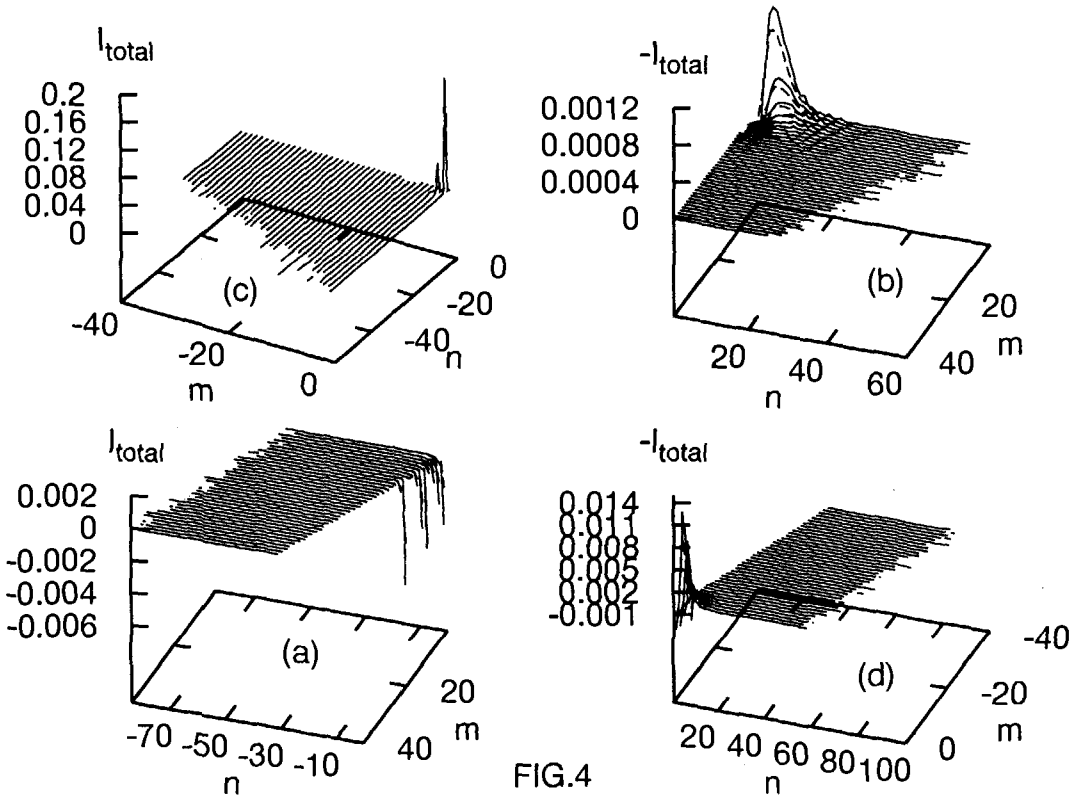
I_{total}
0.2
0.16
0.12
0.08
0.04
0
(c)
-40
-20
0
m
0
-20
-40
n
$-I_{total}$
0.0012
0.0008
0.0004
0
(b)
20
40
60
n
20
40
m
I_{total}
0.002
0
-0.002
-0.004
-0.006
(a)
-70
-50
-30
-10
n
20
40
m
$-I_{total}$
0.014
0.011
0.008
0.005
0.002
-0.001
(d)
20
40
60
80
100
n
-40
-20
0
m

FIG.4

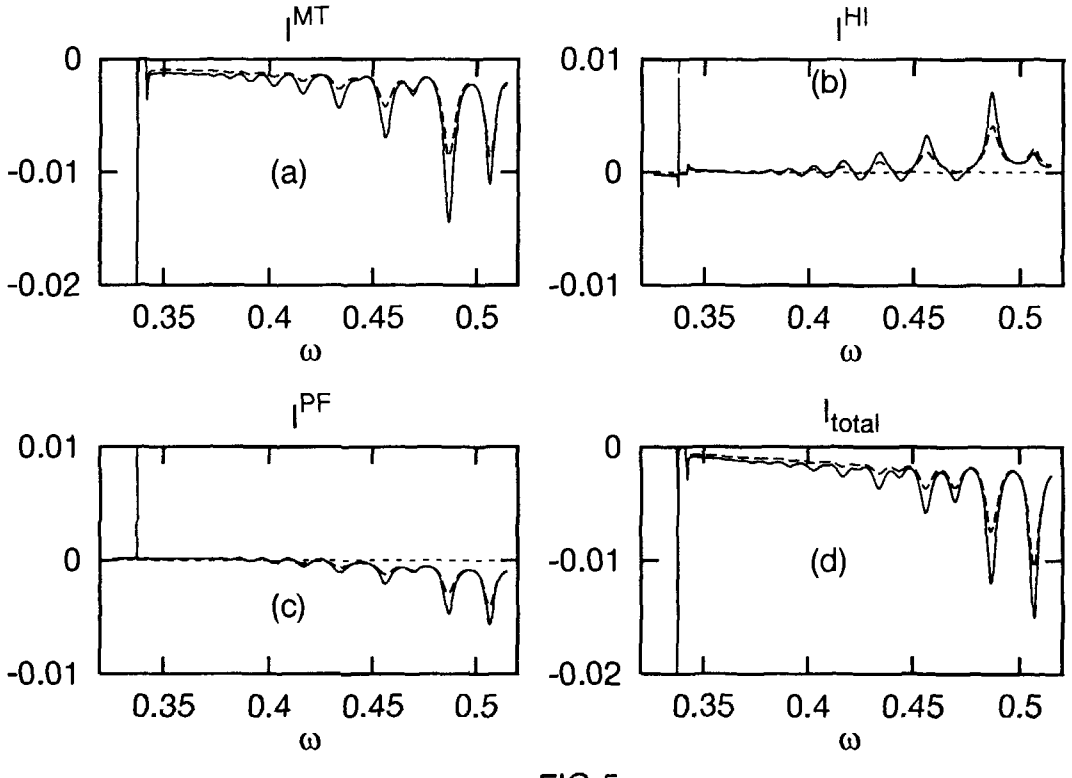
I^{MT}
0
-0.01
-0.02
(a)
0.35
0.4
0.45
0.5
ω
I^{HI}
0.01
0
-0.01
(b)
0.35
0.4
0.45
0.5
ω
I^{PF}
0.01
0
-0.01
(c)
0.35
0.4
0.45
0.5
ω
I_{total}
0
-0.01
-0.02
(d)
0.35
0.4
0.45
0.5
ω

FIG.5